AIAA 80-0687R

Instability of Composite Panels

M. L. Becker*
Air Force Flight Dynamics Laboratory, Wright-Patterson AFB, Ohio
A. N. Palazotto†
Air Force Institute of Technology, Wright-Patterson AFB, Ohio
and
N. S. Khot‡
Air Force Flight Dynamics Laboratory, Wright-Patterson AFB, Ohio

An analytical and experimental program was conducted to study the instability of 8-ply laminated cylindrical panels (graphite-epoxy) subjected to an axial compressive loading. The analysis included three different ply orientations, five different boundary conditions on the vertical edges, and three different panel sizes. The analytical buckling loads were obtained by using the linear bifurcation branch of the STAGS-C computer code. Several nonlinear collapse analyses were also made on selected configurations. The experimental tests were conducted by the Air Force Flight Dynamics Laboratory using a specially designed test fixture. Good agreement was obtained between the analytical and experimental buckling loads, particularly when the nonlinear collapse load was used. The linear bifurcation results were 11-28% higher than the nonlinear results, indicating that the nonlinear effects in circular composite panels are important. The boundary conditions had the greatest influence on the buckling load, followed by the aspect ratio, and finally ply orientation. The (±45)2s panels exhibited an unusually large increase in the buckling load when the aspect ratio was small and the in-plane displacements were restrained at the edges.

Nomenclature

C	= chord length
E_1	= longitudinal modulus of elasticity
E_2	= transverse modulus of elasticity
G_{12}	= shear modulus
L	= panel length
N_x	= force resultant in x direction
R	= panel radius
t	= panel thickness
u,v,w	= displacements in x,y,z directions, respectively
x,y,z	= structural coordinate directions
θ	= ply orientation
ν	= Poisson's ratio
$w_{,x}$	= comma denotes partial differentiation with respect to subscript

Introduction

FIBER-reinforced composites have become increasingly more important in weight-sensitive applications such as aircraft and space vehicles. However, the tremendous advantages of these materials cannot be exploited until the material and its failure mechanisms are fully understood.

One common structural component in these vehicles that must be investigated is the curved panel. Although much work has been done on isotropic curved panels and on composite circular cylinders, very little information is available on the buckling of composite curved panels. Rehfield and Hallauer[1] and Sobel,[2] in their work on isotropic curved panels, found that the buckling stress was sensitive to rotational, circumferential, and longitudinal restraints of the unloaded edges, in decreasing order of influence. They also found that these edge conditions had a much greater influence on the buckling loads than material imperfections.

One investigation of the primary buckling behavior of composite curved panels was conducted by Wilkins,[3] who studied the effects of ply orientation and R/t ratio. He found that laminated composite panels suffer from imperfection sensitivity and that composite shells could snap through and return to their original shape when the bifurcation load was removed. Wilkins' work was limited to one panel size and two boundary conditions on the unloaded edges. This paper looks at different ply orientations, more boundary conditions, and several panel sizes to determine their effects on the buckling load.

Experimental Procedure

All test specimens were 8-ply laminated panels with the same thickness and curvature. Figure 1 shows the panel geometry and coordinate systems. The specimens were hand-laid into 17×36-in. panels using T300/5208 graphite epoxy and later cut to the required test size. The material properties were determined experimentally to be

$$E_1 = 20.5 \times 10^6 \text{ psi} \qquad E_2 = 1.3 \times 10^6 \text{ psi}$$

$$G_{12} = 0.75 \times 10^6 \text{ psi} \qquad \nu_{12} = 0.335$$

The test fixture, furnished by the Air Force Flight Dynamics Laboratory, provided a clamped boundary condition on the curved edges and either a simple support or free boundary condition on the straight edges. The side supports of the fixture are shown in Fig. 2. The edge of the test specimen was inserted between the two inner bars which held the specimen with thin, knife-like edges and allowed the specimen to rotate in the $w_{,y}$ direction and to move in the u and v directions. The side supports were removed entirely to provide the free edge boundary condition.

The tests were conducted on a 20,000 lb Instron testing machine, using the following assembly procedure: 1) the base plate of the fixture was placed on the load cell, 2) the test panel was installed in the base plate and side supports, 3) the

Presented as Paper 80-0687 at the AIAA/ASME/ASCE/AHS 21st Structures, Structural Dynamics and Materials Conference, Seattle, Wash., May 12-14, 1980; submitted May 29, 1980; revision received Feb. 20, 1981. This paper is declared a work of the U.S. Government and therefore is in the public domain.

*Former Graduate Student; Captain USAF.

†Professor, Aeronautics and Astronautics Department. Member AIAA.

‡Aerospace Engineer.

top plate was attached to the panel making sure that it was aligned with the bottom plate and that the top plate remained horizontal, and 4) the top plate of the fixture and the loading ram where clamped together to prevent any tilting during the loading cycle. The loading rate was approximately 0.05 in. per min with the load and end shortening being recorded two times per second. When the first buckle occurred, the location was noted and the loading was continued until the top plate contacted the side supports, or until sufficient postbuckling had occurred.

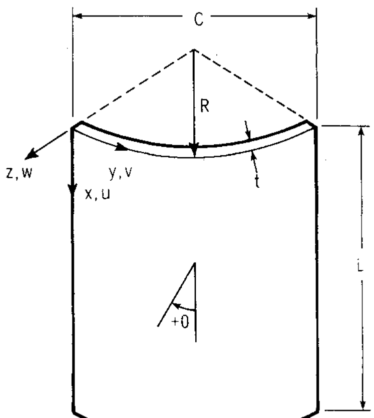

Fig. 1 Panel geometry and coordinate system: $R=12$ in., $t=0.04$ in., 8 – plies approximately 0.005 in., and C is the chord length.

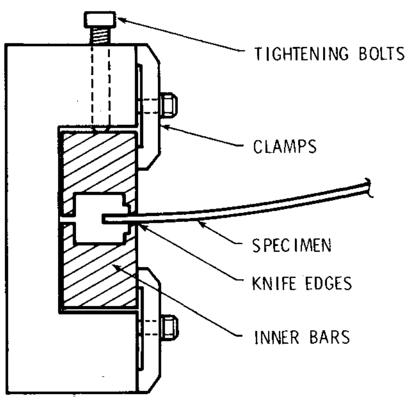

Fig. 2 Top view of fixture side support.

Analytical Approach

The analytical solutions for the buckling loads were obtained by using the STAGS-C computer code, which employs two-dimensional finite-difference approximations of the total potential energy. The bifurcation buckling branch with linear prebuckling analysis was incorporated (45 total runs), but several nonlinear collapse analyses were made on selected configurations to insure that the bifurcation results were good approximations. A convergence analysis consisting of many trial computer runs indicated an ideal grid size of approximately 0.5×0.5 in. A smaller mesh size did not change the buckling load significantly, while a larger mesh size did not result in 5 nodes per ½ sine wave of the buckling pattern (which was found necessary for accurate solutions).

Since difficulty arose in determining whether the desired experimental boundary conditions were actually achieved on the straight edges of the panel, the analytical boundary conditions of these edges were chosen so that they would bound the possible experimental conditions. The boundary conditions chosen are given in Table 1. Each panel configuration was evaluated five times, once for each boundary condition. These analyses include the most rigid and the most flexible conditions that could physically exist. For the curved edges, experimental boundary conditions were much more predictable (securely clamped). Thus, the analytical curved edge boundary conditions were assumed fully clamped (on the top edge, $u=$ free to allow for loading). Boundary conditions were assumed to be the same for prebuckling and buckling.

All of the bifurcation analyses were made assuming no material or geometry imperfections. It was necessary, however, to introduce a small imperfection into the nonlinear analysis to trigger the buckling mode. The imperfection was introduced by applying a small lateral load in the center of the panel. The magnitude of the load was chosen to produce a lateral displacement in the center of the panel of approximately 5% of the panel thickness.

Table 1 Boundary conditions

Type	u	v	w	$w_{,y}$
Free	Free	Free	Free	Free
CC1	Free	Free	0	0
CC4	0	0	0	0
SS1	Free	Free	0	Free
SS4	0	0	0	Free

Table 2 Buckling results

Panel size $C \times L$, in.	Vert. edge B.C.[a]	Nondimensional buckling load $N_x L^2/t^3 E_1$ (±45)2s BIF[b]	(±45)2s NL[c]	(±45)2s EXP[d]	(90, ±45,0)s BIF	(90, ±45,0)s NL	(90, ±45,0)s EXP	(90,0)2s BIF	(90,0)2s NL	(90,0)2s EXP
	Free	12.0			14.5			10.7		
	CC1	44.1			46.0			36.7		
8×12	CC4	68.8			58.2			50.3		
	SS1	40.8			45.7			32.0		
	SS4	66.0			57.5			49.2		
	Free	12.8	10.7		15.1			11.4		
	CC1	43.0			45.6			34.4		
12×12	CC4	54.5			52.6			40.3		
	SS1	42.9	32.5	28.5	45.4	32.5	25.0	33.3	29.5	24.5
	SS4	52.3			52.1			39.6		
	Free	12.8		9.8	15.2		11.3	11.5		8.3
	CC1	42.6			45.2			33.5		
16×12	CC4	40.7			49.5			36.0		
	SS1	42.5			45.2			33.1		
	SS4	38.9			49.3			35.8		

[a]Boundary condition. [b]BIF = bifurcation analysis. [c]NL = nonlinear collapse analysis with 5% of thickness imperfection. [d]EXP = experimental value.

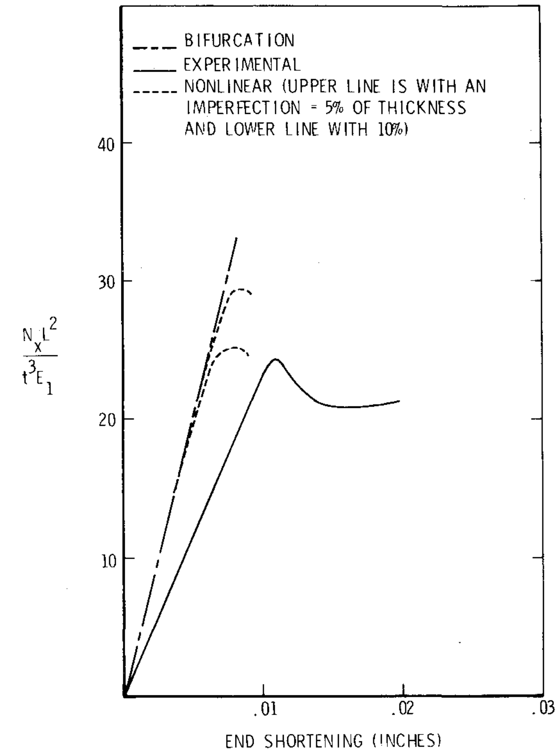

Fig. 3 12×12 (90,0)2s panels with SS1 boundary condition.

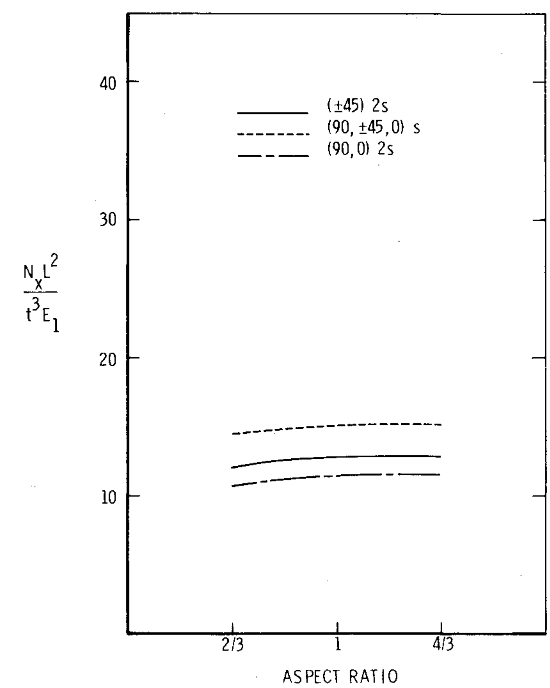

Fig. 4 Bifurcation results for free-edge boundary.

It is recognized by the authors that initial imperfections, both material as well as geometric, can influence the experimental findings. In order to evaluate the actual effect of a given knock-down factor for particular panels, it would be necessary to carryout extensive transverse surface measurements and incorporate them within a nonlinear analysis. The resulting difference depicted in Table 2 can mainly be attributed to the initial imperfections present within given panels.

Results

Three ply orientations, three panel sizes, and five boundary conditions on the vertical edges were analyzed.

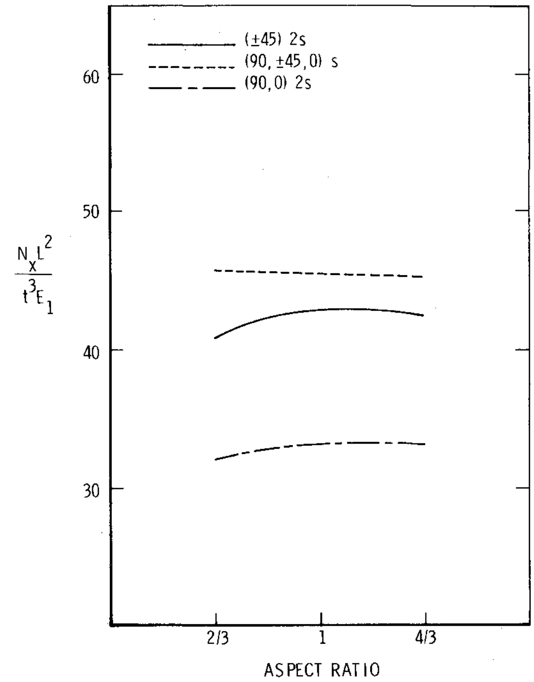

Fig. 5 Bifurcation results for SS1 boundary.

Ply Orientations:

(±45)2s, (90, ±45,0)s, (90,0)2s

Panel sizes (chord length vs height):

8×12, 12×12, 16×12

Boundary conditions (see Table 1):

Free, CC1, CC4, SS1, SS4

The radius of curvature and panel thickness were held constant at 12 and 0.04 in., respectively. A STAGS-C bifurcation analysis was completed for each of the 45 panel configurations and a nonlinear collapse analysis on four configurations. Six configurations were tested experimentally (two panels of each configuration were tested and the average buckling load reported).

The experimental and analytical results are presented in Table 2. The bifurcation buckling loads were from 23 to 34% higher than the experimental buckling loads, except for the (90, ±45,0)s 12×12 panel, which was 45% higher. The larger difference for the latter panel was most likely caused by improper fixture alignment during the experimental test. This conclusion was based on two observations. First, unlike the other panels, the (90, ±45,0)s 12×12 panels both broke (splintered and delaminated) between the top horizontal plate and the vertical side support on one side, indicating a misalignment of the load in the vertical direction. Second, the analytical results for the SS1 boundary condition and the free-edge experimental results show that the (90, ±45,0)s orientation is stronger than the other configurations. The panel in question, however, buckled at a lower load experimentally than the (±45)2s panel, thereby indicating again some anomaly in that particular test.

The nonlinear collapse loads compared more favorably with the experimental results. The results were within 17% of the experimental buckling loads except for the (90, ±45,0)s 12 × 12 panels, which were again higher due to the discrepancy previously discussed. The nonlinear/experimental differences become even less when the size of the imperfection in the analytical analysis is increased as shown in Fig. 3.

Although only four nonlinear analyses were made, it appears that the linear bifurcation results may not yield good

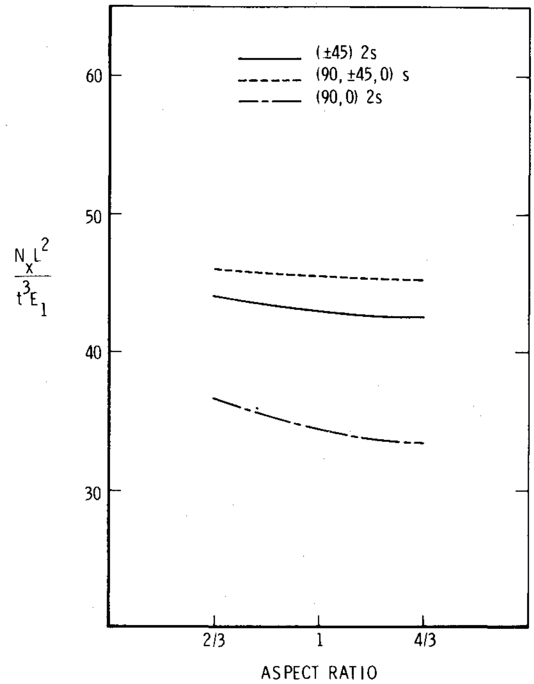

Fig. 6 Bifurcation results for CC1 boundary.

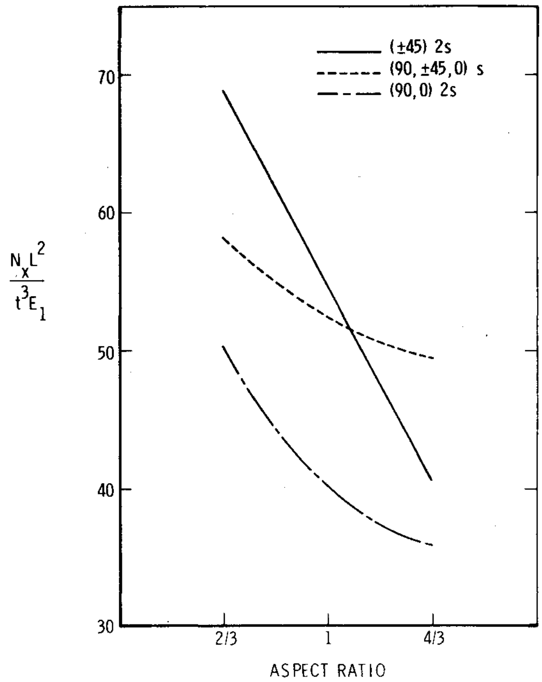

Fig. 8 Bifurcation results for CC4 boundary.

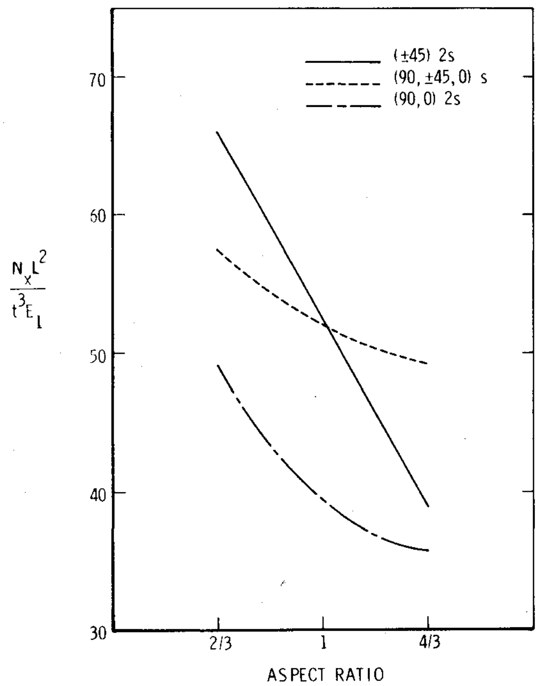

Fig. 7 Bifurcation results for SS4 boundary.

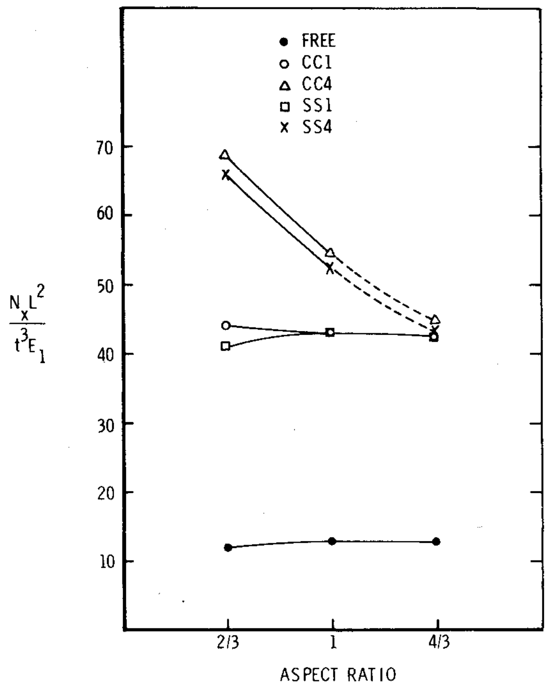

Fig. 9 Bifurcation results for (±45)2s panels.

approximations in all cases. When ±45-deg angle plies were involved, the bifurcation results were as much as 28% higher than the nonlinear results.

In order to study the effects of different boundary conditions, ply orientations, and aspect ratios, the nondimensional bifurcation buckling loads, N_xL^2/t^3E_l were plotted vs the aspect ratio C/L (Figs. 4-11). From the graphs it is apparent that the free-edge panels are significantly weaker than the other panels, as expected. In addition, the in-plane boundary conditions are important, particularly for small aspect ratios where the buckling load can increase as much as 38% when u and v are restrained. The rotational boundary conditions $(w,_y)$ had very little effect on the buckling load as evidenced by the closeness of the CC1/SS1 and CC4/SS4 curves in Figs. 9-11.

One unique point deserves special consideration here. Since the CC4/SS4 boundary conditions produce a stiffer panel than the CC1/SS1 boundary conditions, one would expect the CC4/SS4 panels to have a higher buckling load. This was true in every case except one, the (±45)2s 16×12 configuration (see Table 2). Since this was not expected, the STAGS-C displacement and stress output were examined more closely. From the data, it was noted that the bending moments were always larger in the (±45)2s panels than in the other panels at the same applied load. Therefore, when the boundaries are far apart and can no longer help stiffen the panel, the (±45)2s panels bend more than the other configurations. This increased bending introduces nonlinear effects that are ignored in the bifurcation analysis. The unexpected data points, then, were thought to be errors in the bifurcation analyses. To

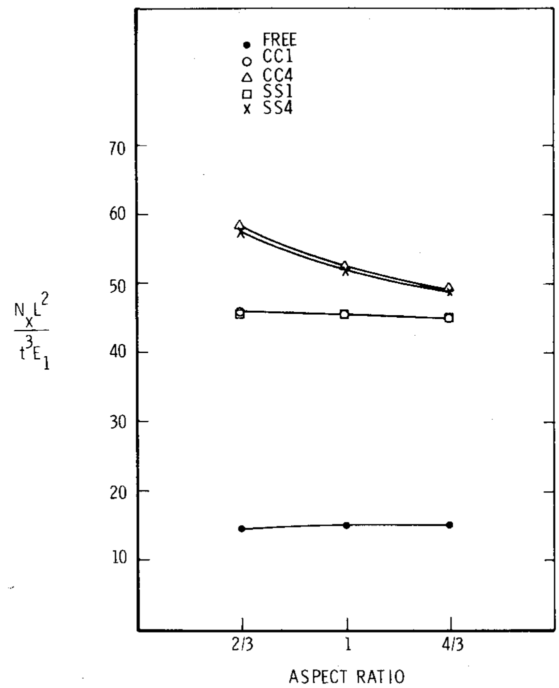

Fig. 10 Bifurcation results for (90, ±45,0)s panels.

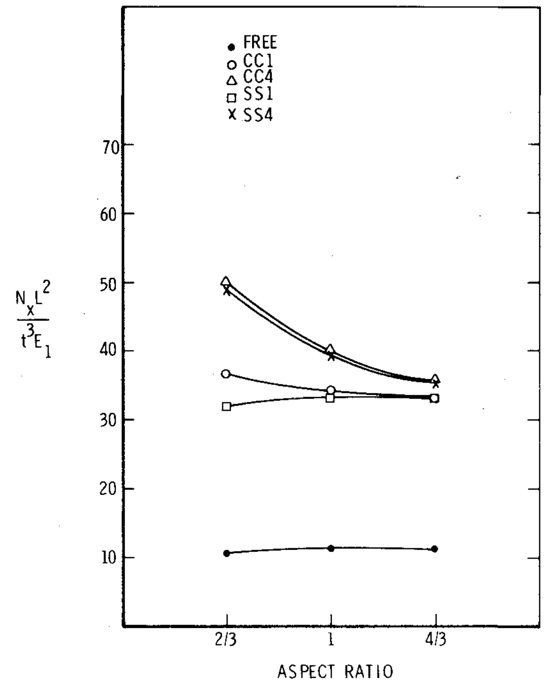

Fig. 11 Bifurcation results for (90,0)2s panels.

verify this, the 16×12 SS1 and SS4 panels were evaluated using the STAGS-C nonlinear collapse analysis. As predicted, the nonlinear analysis showed that the panel with the SS4 boundary condition was stronger than the panel with the SS1 boundary condition (by 1%) and that the bifurcation results were incorrect. This only applies to large aspect ratios and to (±45)2s panels which have less resistance to bending. The SS4 and CC4 curves shown in Fig. 9 reflect this correction by remaining above the SS1 and CC1 curves at the larger aspect ratio (dashed lines).

The effects of different ply orientations are quite apparent from Figs. 4-9. The (90, ±45,0)s panels had the highest buckling loads for every configuration except the (±45)2s panels with CC4 and SS4 boundaries and small aspect ratios. For small aspect ratios and with v restrained at the boundaries, the panel stiffness in the y direction becomes very important. Since all eight plies of the (±45)2s panels contribute to the circumferential stiffness, the stiffness is apparently greater than that of the six plies contributing to the (90, ±45,0)s circumferential stiffness, resulting in a higher buckling load for the (±45)2s panels. When the vertical boundaries are far apart, or when the v displacement is unrestrained, this effect is greatly reduced.

The (90,0)2s panels were weaker than the other two orientations in every case, from as little as 10% for free edges to as much as 30% for restrained edges.

The aspect ratio has very little effect on free, SS1, and CC1 panels, although some changes become evident at aspect ratios below one. There is a drastic effect on the CC4 and SS4 panels as seen in Figs. 7 and 8. This was expected since the boundary condition effects become more prevalent when the supports are close and the in-plane displacements are restrained.

It may be appropriate at this time to suggest a comparison between the buckling load for flat and curved composite panels. Since the boundary condition is so important for the final instability results, it would be necessary to carryout further computations, considering the flat panel with the associated end conditions, such that a valid reference between the given shapes can be established.

Conclusions

The STAGS-C nonlinear collapse analysis (with small imperfection) compared very favorably with experimental results—within 17%. The linear bifurcation results, however, were 11-28% higher than the nonlinear results and up to 34% higher than experimental results, indicating that the bifurcation analysis does not always yield a good approximation of the buckling load.

The boundary conditions have the greatest influence on the buckling load, followed by the aspect ratio, and finally the ply orientation. The out-of-plane displacement w was the most critical boundary condition, but the in-plane displacements u and v also affected the buckling load by as much as 38%. When the vertical edges were free, neither the aspect ratio nor ply orientation had a significant effect. The aspect ratio influenced the buckling load significantly, but only when the in-plane displacements at the vertical edges were restrained. The (90,0)2s panels buckled at a lower value than the other configurations in all analytical and experimental cases, indicating the angle plies are needed for strength.

The strength of the (±45)2s panels increased dramatically when the aspect ratio was small and the in-plane displacements were restrained at the edges. This effect was present in the other ply orientations, but much less pronounced.

References

[1] Rehfield, L.W. and Hallauer, W.L. Jr., "Edge Restraint Effect of Buckling of Compressed Curved Panels," *AIAA Journal,* Vol. 6, Jan. 1968, pp. 187-189.

[2] Sobel, L.H., Weller, T., and Agarwal, B.L., "Buckling of Cylindrical Panels Under Axial Compression," *Computer and Structures,* Vol. 6, Feb. 1976, pp. 29-35.

[3] Wilkins, D.J., "Compression Buckling Tests of Laminated Graphite-Epoxy Curved Panels," AIAA Paper 74-32, presented at the AIAA 12th Aerospace Sciences Meeting, Washington, D.C., Jan. 30-Feb. 1, 1974.